packing is mainly determined by N–H···O hydrogen bonds involving the N–H group from the base and the oxygen atom from THF [N3···O1′, 2.866 (9) Å; N3–H9···O1′, 175 (prime indicates $1 - x$, $1 - y$, $1 - z$)].

A few structural conclusions can be drawn from the structural data reported above which are in agreement with those from the literature:[1] moving from tricoordinate copper(I) (complexes **5** and **6**) to tetracoordinate copper(I) (complexes **3** and **4**) the Cu–I and, by a lesser extent, Cu–N bond lengths increase as a consequence of the increasing coordination number, independently of the structural form (Table VII). The Cu···Cu separation seems to be strictly related to the structural form, the lower value being observed for the tricoordinate dimer, **6**. In addition moving from the $(CuIL)_2$ dimer (**6**) to the $CuIL_2$ monomer (**5**) a significant decrease in the Cu–I distances is observed, as expected. There is no significant difference in the Cu–N distances for **5** and **6**. The range of the I···I separations is rather narrow (Table VII).

Contribution from the Departments of Chemistry, University of Florence, Florence, I-50144 Italy, and University of Siena, Siena, Italy, ISSECC (CNR), Florence, Italy, and Facultad de Ciencias Quimicas, University of Valencia, Valencia, Spain

Anion Coordination Chemistry. 2.[1] Electrochemical, Thermodynamic, and Structural Studies on Supercomplex Formation between Large Polyammonium Cycloalkanes and the Two Complex Anions Hexacyanoferrate(II) and Hexacyanocobaltate(III)

Andrea Bencini,[2a] Antonio Bianchi,[2b] Enrique Garcia-España,[2c] Mauro Giusti,[2a] Stefano Mangani,[2d] Mauro Micheloni,*[2a] Pierluigi Orioli,[2a] and Piero Paoletti*[2a]

The stability constants of 1:1 "supercomplexes" formed between the three large, variously protonated, polyazacycloalkanes 1,4,7,10,13,16,19,22,25-nonaazacycloheptacosane (L1), 1,4,7,10,13,16,19,22,25,28-decaazacyclotriacontane (L2), and 1,4,7,10,13,16,19,22,25,28,31-undecaazacyclotritriacontane (L3) and the anions $[Fe(CN)_6]^{4-}$ and $[Co(CN)_6]^{3-}$ have been determined by potentiometry at 25 °C in 0.15 NaClO$_4$. Many species are formed, and the anion $[Fe(CN)_6]^{4-}$ forms "supercomplexes" that are more stable than the corresponding species involving the less charged anion $[Co(CN)_6]^{3-}$. In the case of "supercomplexes" involving $[Fe(CN)_6]^{4-}$, the CV technique was applied to confirm potentiometric studies. Results are discussed assuming that Coulombic forces are the most important factor which governs the formation of these "supercomplexes". The molecular structure of the "supercomplex" $[H_8L2][Co(CN)_6]_2Cl_2 \cdot 10H_2O$ has been determined by single-crystal X-ray analysis. The compound crystallizes in the $P\bar{1}$ space group with $a = 14.818$ (3) Å, $b = 10.414$ (2) Å, $c = 8.974$ (2) Å, $\alpha = 78.68(1)°$, $\beta = 85.99$ (1)°, $\gamma = 89.67$ (2)°, and $Z = 1$. Refinement of the atomic parameters by least squares gave a final R factor of 0.075 ($R_w = 0.074$) for 3178 unique reflections having $I > 3\sigma(I)$. The structure consists of discrete $(H_8L2)^{8+}$ cations, $[Co(CN)_6]^{3-}$ anions outside the macrocyclic cavity, chloride anions, and water molecules. The macrocycle displays an elongated elliptical shape, and its conformation appears essentially imposed by the strong Coulombic repulsions between the positively charged nitrogen atoms, which form two stiff parallel chains. There are two unprotonated nitrogen atoms on opposite sides of the cycle. Several hydrogen bonds are formed between the cyanide groups of one of the hexacyanocobaltate(III) anions and the macrocyclic nitrogen atoms. The hydrogen-bonding scheme is completed by several other bonds involving chloride anions and water molecules.

Introduction

Anion coordination chemistry is a rapidly growing research field.[3–5] This type of investigation has been shown important in many biological processes and synthetic chemistry.[6,7] Since most anions exist only in a limited pH range, the cationic counterparts should exist in the same interval. It has been assumed that polyazamacrocycles are especially suitable for selective binding of inorganic and organic anions, and some evidences have been reported in the last few years.[1,8,9] The cyclic molecular topology and the ability to bind many hydrogen ions enable large polyazacycloalkanes to concentrate positive charge in their polyprotonated form and strongly interact with anionic species. When the anionic species are metal complexes like $[M^{n+}(CN)_6]^{(6-n)-}$ (M = Fe(II), Fe(III), Co(III), Ru(III), etc.) the expression "supercomplexes" has been used[10,11] to describe the second-sphere coordination between the above anions and polyammonium macrocyclic receptors.

In the present work we wish to elucidate the influence of the size of the macrocyclic cavity as well as of the electrostatic charges on the complexation reactions between the series of large polyazacycloalkanes 1,4,7,10,13,16,19,22,25-nonaazacycloheptacosane ([27]aneN$_9$), 1,4,7,10,13,16,19,22,25,28-decaazacyclotriacontane ([30]aneN$_{10}$), and 1,4,7,10,13,16,19,22,25,28,31-undecaazacy-

(1) Part 1: Bianchi, A.; Garcia-España, E.; Micheloni, M.; Paoletti, P. *Inorg. Chem. Acta* **1985**, *102*, L9.
(2) (a) University of Florence. (b) ISSECC. (c) University of Valencia. (d) University of Siena.
(3) Lehn, J. M. *Acc. Chem. Res.* **1978**, *11*, 49. Dietrich, D.; Fyles, D.; Fyles, T.; Lehn, J. M. *Helv. Chim. Acta* **1979**, *62*, 2763. Cullinane, J.; Gelb, R. I.; Margulis, T. N.; Zompa, L. J. *J. Am. Chem. Soc.* **1982**, *104*, 3048. Gelb, R. I.; Lee, B. T.; Zompa, L. J. *J. Am. Chem. Soc.* **1985**, *107*, 909.
(4) Dietrich B. *Inclusion Compounds*; Academic: London, 1984, pp 337–405 and references therein.
(5) Colquhoun, H. M.; Stoddart, J. F.; Williams, D. J. *Angew. Chem., Int. Ed. Engl.* **1986**, *25*, 487 and references therein.
(6) Kimura, E.; Sakonaka, A.; Yatsunami, T.; Kodama, M. *J. Am. Chem. Soc.* **1981**, *103*, 3041. Kimura, E.; Kodama, M.; Yatsunami, T. *Ibid.* **1982**, *104*, 3182.
(7) Hosseini, M. W.; Lehn, J. M. *J. Am. Chem. Soc.* **1982**, *104*, 3525. Hosseini, M. W.; Lehn, J. M. *J. Chem. Soc., Chem. Commun.* **1985**, 1155.

(8) Dietrich, B.; Hosseini, M. W.; Lehn, J. M.; Session, R. B. *J. Am. Chem. Soc.* **1981**, *103*, 1282.
(9) Manfrin, M. F.; Sabbatini, N.; Moggi, L.; Balzani, V.; Hosseini, M. W.; Lehn, J. M. *J. Am. Chem. Soc.* **1985**, *107*, 6888.
(10) Peter, F.; Gross, M.; Hosseini, M. W.; Lehn, J. M.; Sessions, R. B. *J. Chem. Soc., Chem. Commun.* **1981**, 1067.
(11) Peter, F.; Gross, M.; Hosseini, M. W.; Lehn, J. M. *Electroanal. Chem.* **1983**, *144*, 279.

Table I. Experimental Details of the Emf Measurements

curve	ligand	init concn, mmol dm⁻³ [Fe(CN)₆]⁴⁻	[Co(CN)₆]³⁻	ligand	HCl	pH range	no. of data points
1	L1	0.1967		0.0979	0.0099	9.0–4.5	38
2	L1	0.1544		0.0729	−0.0060	9.1–4.4	32
3	L2	0.1961		0.0935	0.0066	9.2–4.4	42
4	L3	0.1608		0.0959	0.0121	9.5–4.1	67
5	L1		0.1591	0.0910	−0.0041	9.2–4.3	69
6	L1		0.1409	0.0951	−0.0224	8.7–2.8	61
7	L2		0.1586	0.0731	−0.0101	8.8–2.8	57
8	L2		0.1359	0.0742	0.0007	8.9–2.8	59
9	L3		0.1963	0.0818	−0.0057	9.2–2.8	76

clotritriacontane ([33]aneN₁₁) (hereafter abbreviated as L1, L2, and L3, respectively) and the anions [Fe(CN)₆]⁴⁻ and [Co-(CN)₆]³⁻.
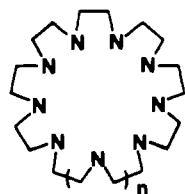
L

n = 1   L = [27]aneN₉

n = 2   L = [30]aneN₁₀

n = 3   L = [33]aneN₁₁

Experimental Section

Materials. All potentiometric measurements were carried out in 0.15 mol dm⁻³ NaClO₄ (C. Erba, ACS grade) purified according to the procedure already described.[12] Standardized CO₂-free solutions of NaOH, used in the potentiometric titrations, were prepared by following the procedure described in ref 13. K₄[Fe(CN)₆]·3H₂O (C. Erba, ACS grade) was used without further purification. K₃[Co(CN)₆] (Aldrich, reagent grade) was recrystallized twice from an ethanol/water mixture. The synthesis of the three compounds L1, L2, and L3 has been reported in ref 14–16, respectively.

Emf Measurements. The potentiometric titrations were carried out by using equipment (potentiometer, buret, stirrer, cell, microcomputer, etc.) that has been fully described.[17] The computer program SUPER-QUAD[18] was used to process data and calculate the equilibrium constants. The basicity constants of macrocycles, necessary in the calculation of the "supercomplex" formation constants, were taken from ref 14–16 for L1, L2, and L3, respectively. In Table I are reported the experimental details of the emf measurements.

Electrochemical Measurements. A classical three-electrode cell was used for electrochemical analysis by cyclic voltammetry. The working electrode was a platinum microsphere, the auxiliary electrode was a platinum disk and the reference electrode was a calomel electrode (SCE). All measurements were carried out at 25 °C in aqueous NaClO₄ (0.15 mol dm⁻³); solutions were carefully deoxygenated with a nitrogen flow.

Preparation of the Crystals. Crystals of the compound [H₈L2][Co-(CN)₆]₂Cl₂·10H₂O, suitable for X-ray analysis, have been obtained by slow evaporation over a period of 3 months at 0 °C a 0.15 mol dm⁻³ NaClO₄ solution containing 2 × 10⁻³ mol dm⁻³ of K₃[Co(CN)₆] and 1 × 10⁻³ mol dm⁻³ of L2·10HCl·2H₂O.[5]

X-ray Crystallography. Crystal data and data collection procedures are summarized in Table II. Cell constants were determined by a

(12) Micheloni, M.; May, P. M.; Williams, D. R. *J. Inorg. Nucl. Chem.* **1978**, *40*, 1209.
(13) Micheloni, M.; Sabatini, A.; Vacca, A. *Inorg. Chim. Acta* **1977**, *25*, 41.
(14) Bencini, A.; Bianchi, A.; Garcia-España, E.; Giusti, M.; Micheloni, M.; Paoletti, P. *Inorg. Chem.* **1987**, *26*, 681.
(15) Bencini, A.; Bianchi, A.; Garcia-España, E.; Giusti, M; Mangani, S.; Micheloni, M.; Orioli, P.; Paoletti, P. *Inorg. Chem.* **1987**, *26*, 1243.
(16) Bencini, A.; Bianchi, A.; Garcia-España, E.; Micheloni, M.; Paoletti, P. *Inorg. Chem.*, in press.
(17) Bianchi, A.; Bologni, L.; Dapporto, P.; Micheloni, M.; Paoletti, P. *Inorg. Chem.* **1984**, *23*, 1201.
(18) Gans, P.; Sabatini, A.; Vacca, A. *J. Chem. Soc., Dalton Trans.* **1985**, 1195.

Table II. Crystal and Data Collection Parameters

formula	C₃₂H₇₈Cl₂Co₂N₂₂O₁₀
fw	1119.9
space group	P1̄
a	14.818 (3) Å
b	10.414 (2) Å
c	8.974 (2) Å
α	78.68 (1) deg
β	85.99 (1) deg
γ	89.67 (2) deg
V	1354.5 Å³
Z	1
D_calcd	1.37 g cm⁻³
λ(Mo Kα)	0.7107 Å; graphite monochromator
cryst dimens	0.42 × 0.17 × 0.15 mm
μ	7.24 cm⁻¹
scan type	θ – 2θ
scan width	(0.9 +0.3 tan θ)°
scan speed	0.05° s⁻¹
data colln range	4° ≤ 2θ ≤ 50°
no. of reflcns colld	4784
no. of reflcns used	3178 (I ≥ 3σ(I))
no. of params	410
Rᵃ	0.075
R_wᵇ	0.074

$^a R = \sum||F_o| - |F_c||/\sum|F_o|$. $^b R_w = [\sum w(|F_o| - |F_c|)^2/\sum w F_o^2]^{1/2}$.

least-squares fitting of 25 accurately centered reflections. Intensity data, collected on a Philips PW automatic diffractometer at room temperature, were corrected for Lorentz, polarization, and absorption effects. Absorption corrections were based on the numerical-integration method, as included in SHELX-76.[19] Maximum and minimum transmission factors were respectively 0.88 and 0.74. The intensities of the reflections −1,2,1, −3,1,0, and −2,2,2 were monitored periodically for stability control during data collection.

The structure was solved by the heavy atom technique, with the use of Patterson and electron density syntheses. The two cobalt(III) ions are located on the centers of symmetry at 0, 0, 0 and ¹/₂, ¹/₂, ¹/₂. The protonated macrocyclic ligand is centrosymmetric at 0, 0, ¹/₂. Refinement was performed by the least-squares technique in two blocks. One block consisted of the hexacyanocobaltate(III) anions and of the non-hydrogen atoms of the macrocyclic ring. The chloride anion, the water oxygen atoms, and the hydrogen atoms of the macrocycle and a water molecule, unambiguously located from a difference Fourier, were refined in the second block. The hydrogen atoms on C(11), C(12), and N(13), which did not refine with acceptable temperature factors, were included in calculated positions and their parameters were not refined. Anisotropic temperature factors were used for all the non-hydrogen atoms. The function minimized was $\sum w(|F_o| - |F_c|)^2$ with weights $w = a/(\sigma^2(F) + bF^2)$, where a and b are adjustable parameters.

All the calculations were performed with the SHELX-76[19] set of programs, which use the analytical approximation for the atomic scattering factors and anomalous dispersion corrections for all the atoms from ref 20. Table III shows the final atomic coordinates with estimated standard deviations obtained from the least-squares inverse matrix.

Results and Discussion

Equilibrium Studies. The species formed and the relative equilibrium constants for the systems [Fe(CN)₆]⁴⁻/HₙLⁿ⁺ and

(19) Sheldrick, G. M. "SHELX-76"; Program for Crystal Structure Determination; University of Cambridge: Cambridge, England, 1976.
(20) *International Tables for X-ray Crystallography*; Kynoch: Birminghan, England, 1974; Vol. IV.

Table III. Atomic Coordinates ($\times 10^4$) with Their Esd's in Parentheses for $[H_8L2][Co(CN)_6]_2Cl_2\cdot 10H_2O$

atom	x/a	y/b	z/c	atom	x/a	y/b	z/c
N(1)	2997 (4)	9319 (5)	3283 (6)	H(19)	−2846 (30)	7441 (43)	9320 (54)
C(2)	2526 (5)	8343 (6)	4515 (8)	H(20)	−4099	7238	11053
C(3)	1514 (5)	8348 (6)	4351 (8)	H(21)	−4147	5764	10372
N(4)	1099 (4)	7415 (5)	5694 (6)	H(22)	−4698	6552	8511
C(5)	106 (5)	7447 (7)	5868 (8)	H(23)	−5021	7726	9615
C(6)	−209 (5)	6550 (7)	7350 (8)	H(24)	−4241	8089	6751
N(7)	−1206 (4)	6566 (5)	7567 (6)	H(25)	−3378	8399	7894
C(8)	−1563 (5)	5690 (7)	9026 (9)	H(26)	−5240 (53)	9774 (73)	7668 (90)
C(9)	−2591 (6)	5684 (8)	9180 (10)	H(27)	−4433 (70)	9915 (98)	8536 (123)
N10)	−2958 (4)	6820 (6)	9771 (8)	H(28)	−4225 (43)	11443 (63)	6326 (76)
C(11)	−3951 (6)	6785 (11)	10080 (14)	H(29)	−4132 (51)	10240 (74)	5371 (90)
C(12)	−4457 (7)	7318 (14)	9042 (14)	Co(1)	0	0	0
N(13)	−4101 (4)	8354 (7)	7817 (7)	C(16)	1025 (4)	573 (6)	851 (7)
C(14)	−4452 (6)	9655 (10)	7805 (10)	N(16)	1633 (4)	972 (5)	1359 (6)
C(15)	−3991 (5)	10623 (8)	6520 (10)	C(17)	264 (5)	−1793 (7)	745 (8)
H(1)	2845 (41)	10054 (60)	3336 (73)	N(17)	375 (5)	−2876 (7)	1201 (8)
H(2)	3011 (104)	8778 (151)	2317 (183)	C(18)	−671 (5)	1 (7)	1856 (8)
H(3)	2803 (39)	7496 (58)	4443 (70)	N(18)	−1080 (5)	−46 (7)	3015 (8)
H(4)	2747 (49)	8596 (72)	5524 (87)	Co(2)	5000	5000	5000
H(5)	1257 (36)	9250 (53)	4427 (65)	C(19)	4300 (5)	3447 (7)	5330 (8)
H(6)	1295 (51)	7900 (74)	3345 (90)	N(19)	3895 (5)	2483 (7)	5535 (8)
H(7)	1204 (39)	6600 (57)	5700 (69)	C(20)	4352 (5)	5763 (7)	3310 (8)
H(8)	1337 (47)	7720 (68)	6488 (83)	N(20)	3983 (4)	6293 (6)	2251 (7)
H(9)	−128 (43)	8195 (63)	5797 (77)	C(21)	5820 (5)	4281 (7)	3682 (8)
H(10)	−170 (38)	7014 (56)	5072 (68)	N(21)	6303 (5)	3830 (7)	2873 (8)
H(11)	−69 (32)	5678 (47)	7250 (56)	Cl	1695 (2)	4856 (2)	4893 (3)
H(12)	54 (40)	6982 (59)	8352 (72)	O(W1)	−2288 (5)	8516 (6)	5485 (6)
H(13)	−1390 (32)	73338 (47)	7504 (57)	H1(w1)	−2612 (55)	8212 (80)	5175 (97)
H(14)	−1437 (50)	6105 (73)	6917 (88)	H2(w1)	−1836 (53)	8825 (77)	4797 (94)
H(15)	−1257 (39)	6113 (56)	9727 (69)	O(w2)	7949 (4)	2931 (5)	1704 (6)
H(16)	−1293 (44)	4842 (65)	9080 (78)	O(w3)	2895 (5)	8207 (7)	673 (7)
H(17)	−2728 (54)	4913 (79)	9793 (101)	O(w4)	1964 (6)	2912 (7)	7824 (7)
H(18)	−2713 (70)	5537 (105)	7985 (132)	O(w5)	3167 (5)	284 (8)	8085 (10)

Table IV. Logarithms of the Equilibrium Constants for the Reactions of "Supercomplex" Formation between the Large Macrocycles L1, L2, and L3 and the $[Fe(CN)_6]^{4-}$ Anion[a]

reaction	log K^b		
	L = L1	L = L2	L = L3
$H_4L^{4+} + [Fe(CN)_6]^{4-} =$ $[H_4LFe(CN)_6]$	4.06 (4)	3.69 (5)	3.61 (3)
$H_5L^{5+} + [Fe(CN)_6]^{4-} =$ $[H_5LFe(CN)_6]^+$	5.63 (4)	4.78 (5)	4.66 (3)
$H_6L^{6+} + [Fe(CN)_6]^{4-} =$ $[H_6LFe(CN)_6]^{2+}$	7.60 (5)	6.23 (6)	5.72 (3)
$H_7L^{7+} + [Fe(CN)_6]^{4-} =$ $[H_7LFe(CN)_6]^{3+}$	9.33 (6)	7.92 (7)	6.93 (4)
$H_8L^{8+} + [Fe(CN)_6]^{4-} =$ $[H_8LFe(CN)_6]^{4+}$		9.03 (8)	8.07 (4)

[a] Experimental conditions: 25 °C; $I = 0.15$ mol dm^{-3} (NaClO$_4$). [b] Values in parentheses are standard deviations in the last significant figure.

$[Co(CN)_6]^{3-}/H_nL^{n+}$ (where L = L1, L2, L3) are reported in Table IV and Table V, respectively. It should be noted that only 1:1 species are formed, and in order to form a "supercomplexed" species, the macrocycle has to be at least tetracharged. The first consideration that can be done is relative to the great number of species formed and their high stability. For the same macrocycle the stability of the "supercomplex" species increases as the macrocycle becomes more protonated (charged). Furthermore, "supercomplexes" formed with the four-charged anionic species $[Fe(CN)_6]^{4-}$ are always much more stable than the corresponding species involving the three-charged species $[Co(CN)_6]^{3-}$. In Table VI the equilibrium constants relative to the reaction of stepwise addition of hydrogen ion to "supercomplexes" have been reported. These results show that the less positively charged supercomplex is always more easily protonated. Furthermore, among supercomplexes with the same stoichiometry (the same *n* in Table VI) the easiest protonation occurs with the largest macrocycle L3. The above general considerations strongly indicate that the interactions which lead to the formation of these rather strong "supercomplexes" are essentially Coulombic in nature. In the case

Table V. Logarithms of the Equilibrium Constants for the Reactions of "Supercomplex" Formation between the Large Macrocycles L1, L2, and L3 and the $[Co(CN)_6]^{3-}$ Anion[a]

reaction	log K^b		
	L = L1	L = L2	L = L3
$H_4L^{4+} + [Co(CN)_6]^{3-} =$ $[H_4LCo(CN)_6]^+$	2.61 (3)	2.03 (4)	2.63 (3)
$H_5L^{5+} + [Co(CN)_6]^{3-} =$ $[H_5LCo(CN)_6]^{2+}$	3.00 (3)	2.10 (4)	3.05 (3)
$H_6L^{6+} + [Co(CN)_6]^{3-} =$ $[H_6LCo(CN)_6]^{3+}$	3.36 (3)	2.37 (4)	3.52 (3)
$H_7L^{7+} + [Co(CN)_6]^{3-} =$ $[H_7LCo(CN)_6]^{4+}$	3.78 (3)	3.23 (4)	4.05 (4)
$H_8L^{8+} + [Co(CN)_6]^{3-} =$ $[H_8LCo(CN)_6]^{5+}$	4.09 (3)	3.66 (4)	4.55 (4)
$H_9L^{9+} + [Co(CN)_6]^{3-} =$ $[H_9LCo(CN)_6]^{6+}$		4.43 (4)	4.87 (5)
$H_{10}L^{10+} + [Co(CN)_6]^{3-} =$ $[H_{10}LCo(CN)_6]^{7+}$			5.32 (5)

[a] Experimental conditions: 25 °C, $I = 0.15$ mol dm^{-3} (NaClO$_4$). [b] Values in parentheses are standard deviations in the last significant figure.

Table VI. Logarithms of the Equilibrium Constants for the Stepwise Protonation Reactions of "Supercomplexes"

$$[H_nLM(CN)_6]^{(n+m-6)+} + H^+ = [H_{n+1}LM(CN)_6]^{(n+m-5)+}$$
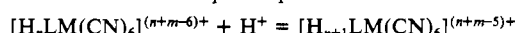
	log K					
	M = Fe(II); $m = +2$			M = Co(III); $m = +3$		
n	L = L1	L = L2	L = L3	L = L1	L = L2	L = L3
4	7.93	8.89	9.13	6.74	7.87	8.50
5	6.18	6.69	7.53	4.57	5.51	6.94
6	4.97	5.53	5.73	3.66	4.70	5.04
7		4.13	4.70	2.62	3.45	4.08
8					2.73	3.07
9						2.68

of $[Fe(CN)_6]^{4-}$ anion there is a clear trend (see Table IV) indicating that the species equally protonated are slightly more stable

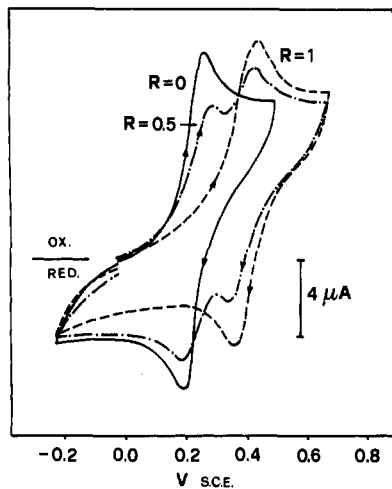**Figure 1.** Effect of increasing amount of L1 on the cyclic voltammograms of $[Fe(CN)_6]^{4-}$ (pH 3.5, scan rate 50 mV s^{-1}). Concentration of $[Fe(CN)_6]^{4-}$ is 1 mmol dm^{-3}. R = mmol of L1/mmol of $[Fe(CN)_6]^{4-}$.

with the smaller macrocycles in which the positive charges are more concentrated and thus more strongly interacting with the anionic species. The same trend is not observed for the less charged anion $[Co(CN)_6]^{3-}$ (see Table V). We interpret these results by assuming that the most important role in the formation of these "supercomplexes" is played by Coulombic forces, as already stated, although other effects, such as hydrogen bonding and macrocycle configuration, should be important and give significant contributions to the overall stability of the supercomplex species.

Considering second-sphere interactions, which involve polyazamacrocycles and anionic complexes, the problem of selecting the species that are present at equilibrium is critical. The supercomplex formation does not influence the UV spectroscopic properties of $[Fe(CN)_6]^{4-}$ and $[Co(CN)_6]^{3-}$ anions,[5] and in the latter case, only the potentiometric technique allows an accurate determination of the equilibrium constants. However, since in the system macrocycle/$[Co(CN)_6]^{3-}$/H$^+$ there are many species whose formation constants differ very slightly, great care has to be taken in the species selection criteria. In the case of the anion $[Fe(CN)_6]^{4-}$ independent electrochemical measurements, such as cyclic voltammetry, can be carried out and the results compared with those obtained from potentiometry. Indeed the supercomplex formation does affect the electrochemical properties of the complex anions $[Fe(CN)_6]^{4-}$ by stabilizing the more highly charged form, i.e. the lower oxidation state of the central metal ion. Solutions of $[Fe(CN)_6]^{4-}$ (1 × 10^{-3} mol dm^{-3}) were studied by cyclic voltammetry in the absence and in the presence of the macrocycles L1, L2, and L3, respectively, as a function of pH. To avoid protonation of the $[Fe(CN)_6]^{4-}$ anion all experiments were carried out at pH higher than 3.5.[21] Increasing amounts of the macrocycle hydrochloride under study and various amounts of NaOH, to keep the pH constant, were added to the starting solution containing the $[Fe(CN)_6]^{4-}$ anion in order to vary the concentration ratio R = mmol of L/mmol of $[Fe(CN)_6]^{4-}$ from 0 to 1 or more, and the CV curves were recorded. In Figure 1 the CV voltammograms obtained with the macrocycle L1 with three R values, 0, 0.5, and 1, have been reported. A second redox signal, which is more anodic with respect to that observed for the uncomplexed $[Fe(CN)_6]^{4-}$/$[Fe(CN)_6]^{3-}$ couple, grows as R increases and becomes unique when R is equal or greater than 1. Similar results were obtained for L2 and L3. These results indicate that with protonated forms of L1, L2, and L3 the $[Fe(CN)_6]^{4-}$ anion forms only 1:1 supercomplex species whose redox potentials are anodically shifted with respect to the uncomplexed anion. The $E_{1/2}$ potential increases as pH decreases, forming steps of definite potential in correspondence with the formation of the supercomplexed species as shown in Figure 2. This figure reports the distribution diagram for the system L1/$[Fe(CN)_6]^{4-}$ and the $E_{1/2}$
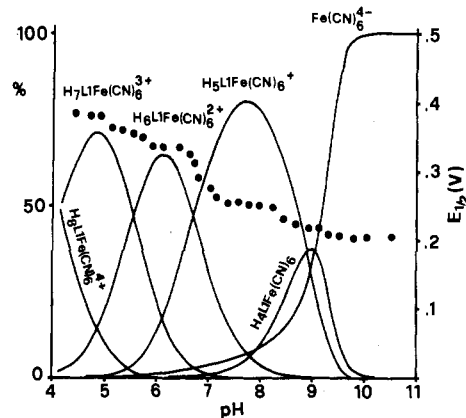
(21) Jordan, J.; Ewing, G. J. *Inorg. Chem.* **1962**, *1*, 587.

Figure 2. Distribution diagram (—) for the system H$^+$/L1/$[Fe(CN)_6]^{4-}$ and $E_{1/2}$ (mV) in CV (●) for the couple (H$_n$L1)$[Fe(CN)_6]^{(n-4)+}$/(H$_n$L1)$[Fe(CNe)_6]^{(n-3)+}$ vs pH.

(mV) values in cyclic voltammetry of the couple (H$_n$L1)[Fe(CN)_6]$^{(n-4)+}$/(H$_n$L1)$[Fe(CN)_6]^{(n-3)+}$ as a function of pH. It can be easily seen that the steps in the $E_{1/2}$ potential, due to the existence of a predominant species in that pH-interval, are coincident with the peaks of the same species found by potentiometric technique. Similar results have been obtained for the two macrocycles L2 and L3. Unfortunately the CV technique cannot be used with $[Co(CN)_6]^{3-}$ because of the electrochemical behavior of this species upon reduction.[22]

If we assume that the anion complexation unit of these macrocycles consists of several positively charged binding sites arranged around the cavity defined by the molecular shape, a good question could be whether the anionic species goes or not inside the macrocyclic cavity. The equilibrium studies of the "supercomplex" formation of the large macrocycles that we have so far investigated do not show any evidence of complexation selectivity. The size of the macrocyclic cavity does not seem to influence much the stability constants. It is interesting to note that especially in the case of $[Fe(CN)_6]^{4-}$ the stabilities of the six-protonated $[H_6LFe(CN)_6)]^{2+}$ (L = L1, L2, L3; see Table IV) and the eight-protonated $[H_8LFe(CN)_6)]^{4+}$ "supercomplexes" are very similar to those found for fully protonated [24]aneN$_6$ and [32]-aneN$_8$ respectively, in which adjacent nitrogen donor atoms are bridged by propylenic chains.[8] In the case of [24]aneN$_6$ the total atomicity and presumably the cavity size are rather different from those of the macrocycles L1, L2, and L3. We explain these results by assuming that the anionic species does not go inside the macrocyclic cavity. In order to further support the above assumption we have determined the crystal structure of the "supercomplex" $[H_8L2][Co(CN)_6]_2Cl_2\cdot10H_2O$. Preliminary results on this structure have been already reported in ref 23.

Description of the Structure. The crystal structure of $[H_8L2][Co(CN)_6]_2Cl_2\cdot10H_2O$ consists of discrete (H$_8$L)$^{8+}$ cations, $[Co(CN)_6]^{3-}$ and chloride anions, and water molecules. As already pointed out, the hexacyanocobaltate(III) anions lie on crystallographic centers of symmetry and show only slight deviations from the O_h octahedral symmetry (Table VII). The protonated macrocyclic ligand also lies on a crystallographic center of symmetry and shows an elongated elliptical shape with the main axes about 15 and 6 Å long (see Figure 3). Its conformation appears essentially imposed by the strong Coulombic repulsions between the positively charged nitrogen atoms N(1), N(4), N(7), and N(13) and their centrosymmetric counterparts. Two stiff parallel chains (N(1)–C(2)–C(3)–N(4)–C(5)–C(6)–N(7) and its symmetry-related one) are in fact formed, with torsion angles between adjacent bonds all close to 180° (Table VII). N(10) and N(10)'

(22) Cotton, F. A.; Wilkinson, G. *Advanced Inorganic Chemistry*, 3rd ed.; Interscience: New York, 1972; p 879.
(23) Bianchi, A.; Garcia-España, E.; Mangani, S.; Micheloni, M.; Orioli, P.; Paoletti, P. *J. Chem. Soc., Chem. Commun.* **1987**, 729.
(24) Johnson, C. K. "ORTEP"; Report ORNL-3794; Oak Ridge National Laboratory: Oak Ridge, TN, 1971.

Table VII. Distances (Å), Angles (deg), and Torsion Angles (deg) with Their Esd's in Parentheses for $[H_8L2][Co(CN)_6]_2Cl_2\cdot10H_2O$

N(1)-C(2)	1.483 (8)	C(2)-C(3)	1.517 (10)	C(3)-N(4)	1.489 (8)
N(4)-C(5)	1.469 (9)	C(5)-C(6)	1.514 (9)	C(6)-N(7)	1.476 (9)
N(7)-C(8)	1.506 (9)	C(8)-C(9)	1.519 (11)	C(9)-N(10)	1.476 (11)
N(10)-C(11)	1.478 (11)	C(11)-C(12)	1.276 (16)	C(12)-N(13)	1.453 (13)
N(13)-C(14)	1.447 (13)	C(14)-C(15)	1.501 (11)	C(15)-N(1)	1.499 (9)
Co(1)-C(16)	1.896 (7)	Co(1)-C(17)	1.903 (7)	Co(1)-C(18)	1.879 (7)
C(16)-N(16)	1.153 (9)	C(17)-N(17)	1.137 (10)	C(18)-N(18)	1.159 (10)
Co(2)-C(19)	1.889 (7)	Co(2)-C(20)	1.891 (7)	Co(2)-C(21)	1.890 (8)
C(19)-N(19)	1.150 (10)	C(20)-N(20)	1.171 (9)	C(21)-N(21)	1.147 (11)

N(1)-C(2)-C(3)	111.1 (5)	C(2)-C(3)-N(4)	106.9 (5)	C(16)-Co(1)-C(17)	92.1 (3)	C(16)-Co(1)-C(18)	88.7 (3)
C(3)-N(4)-C(5)	114.7 (5)	N(4)-C(5)-C(6)	108.6 (6)	C(17)-Co(1)-C(18)	88.1 (3)	Co(1)-C(16)-N(16)	177.2 (6)
C(5)-C(6)-N(7)	110.0 (6)	C(6)-N(7)-C(8)	112.7 (5)	Co(1)-C(17)-N(17)	176.5 (7)	Co(1)-C(18)-N(18)	177.5 (6)
N(7)-C(8)-C(9)	111.3 (6)	C(8)-C(9)-N(10)	112.4 (7)	C(19)-Co(2)-C(20)	91.9 (3)	C(19)-Co(2)-C(21)	89.4 (3)
C(9)-N(10)-C(11)	114.1 (7)	N(10)-C(11)-C(12)	119.8 (9)	C(20)-Co(2)-C(21)	89.5 (3)	Co(2)-C(19)-N(19)	178.2 (7)
C(11)-C(12)-N(13)	120.1 (9)	C(12)-N(13)-C(14)	116.7 (8)	Co(2)-C(20)-N(20)	176.3 (6)	Co(2)-C(21)-N(21)	178.5 (7)
N(13)-C(14)-C(15)	110.4 (7)	C(14)-C(15)-N(1)	110.3 (7)				

C(15)-N(1)-C(2)-C(3)	176.8	C(5)-C(6)-N(7)-C(8)	179.9	N(10)-C(11)-C(12)-N(13)	-23.6
N(1)-C(2)-C(3)-N(4)	-175.9	C(6)-N(7)-C(8)-C(9)	-177.6	C(11)-C(12)-N(13)-C(14)	-111.1
C(2)-C(3)-N(4)-C(5)	170.4	N(7)-C(8)-C(9)-N(10)	-82.0	C(12)-N(13)-C(14)-C(15)	177.5
C(3)-N(4)-C(5)-C(6)	-174.6	C(8)-C(9)-N(10)-C(11)	-174.3	N(1)'-C(15)-C(14)-N(13)	-61.9
N(4)-C(5)-C(6)-N(7)	179.6	C(9)-N(10)-C(11)-C(12)	-91.2	C(14)-C(15)-N(1)'-C(2)'	-178.5

Table VIII. Hydrogen-Bond Distances (Å) Involving the Macrocyclic Nitrogen Atoms

N(1)···O(W3)	2.827	N(7)···N(16)	2.961
N(1)···O(W1)	2.887	N(7)···O(W1)	2.972
N(1)···N(16)	3.051	N(7)···Cl(1)	3.018
N(4)···O(W2)	2.774	N(10)···O(W4)	2.755
N(4)···Cl(1)	3.006	N(10)···N(16)	3.005
N(4)···N(18)	3.177	N(13)···N(19)	3.286
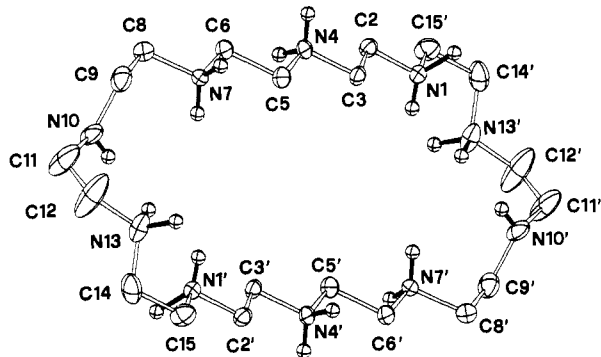
Figure 3. ORTEP[24] drawing of the octaprotonated form of the 1,4,7,10,13,16,19,22,25,28-decaazacyclotriacontane ring showing the atom labeling and the hydrogen atoms bonded to the ring nitrogens. The thermal ellipsoids are drawn at 30% probability, and the hydrogen atoms are shown as spheres of arbitrary radius.

Figure 4. ORTEP[24] view of a portion of the crystal packing showing the $[H_8L2]^{8+}$ cations (A) and the hexacyanocobaltate(III) anions (B and C) together with the hydrogen bonds between them. The thermal ellipsoids are drawn at 30% probability.

are the only unprotonated nitrogen atoms of the ring, as clearly shown by a difference Fourier map.

The macrocyclic nitrogen atoms form several hydrogen bonds with the water molecules, the chloride ions, and the nitrogen atoms of the hexacyanocobaltate(III) anions (Table VIII). The latter bonds are by far the most interesting ones. In this respect, it must be pointed out that the interactions of the macrocyclic cation with the two complex anions are quite different. Eight macrocyclic nitrogen atoms (N(1), N(4), N(7), and N(10) and their centrosymmetric counterparts) are involved in rather strong hydrogen bonds with N(16) and N(18) and their symmetry related atoms, belonging to the hexacyanocobaltate(III) anions at 0, 0, 0 (Figure 4). N(13) and N(13)' form two weak hydrogen bonds (3.286 Å) with N(19) and N(19)' belonging to the hexacyanocobaltate(III) anions at $^1/_2$, $^1/_2$, $^1/_2$.

Extensive hydrogen bonding also involves the water molecules and the chloride ions. The crystal packing of the macrocyclic cations and of the hexacyanocobaltate(III) anions can be described in terms of parallel chains ···A···B···A···B··· (A and B are the cation and the complex anion at 0, 0, 0, respectively) cross-linked by ···A···C··· weaker hydrogen bonds (C is the hexacyanocobaltate(III) anion at $^1/_2$, $^1/_2$, $^1/_2$) (Figure 5).

Figure 5. Stereoview of the crystal packing of the compound $[H_8L2]\cdot[Co(CN)_6]_2Cl_2\cdot10H_2O$ (water molecules and chloride anions omitted for clarity).

Conclusions. Equilibrium and electrochemical studies in aqueous solution, on the binding of the complex anions [Fe-

(CN)$_6$]$^{4-}$ and [Co(CN)$_6$]$^{3-}$ to polyammonium macrocycles of different sizes, show the absence of any selectivity and are consistent with strong interactions, mainly Coulombic in nature, between the anion and the protonated second-sphere ligand. The crystal structure of one of these "supercomplexes" proves that (i) the anionic species [Co(CN)$_6$]$^{3-}$ does not go inside the macrocyclic cavity, (ii) the rigid conformation of the macrocyclic ring is essentially determined by electrostatic repulsions and very likely maintained in solution, and (iii) electrostatic interactions and hydrogen bonds between the cationic and anionic species have a synergistic effect in the supercomplex formation.

Contribution from the Department of Chemistry, University of Hong Kong, Hong Kong, and Contribution No. 7597 from the Arthur Amos Noyes Laboratory, California Institute of Technology, Pasadena, California 91125

Triphenylphosphine Reduction of Dioxoosmium(VI) Porphyrins. Crystal Structures of Bis(triphenylphosphine oxide)(octaethylporphinato)osmium(II) and Bis(triphenylphosphine)(*meso*-tetraphenylporphinato)osmium(II)

Chi-Ming Che,*[1a] Ting-Fong Lai,[1a,c] Wai-Cheung Chung,[1a] William P. Schaefer,[1b] and Harry B. Gray[1b]

Received September 18, 1986

The reactions of Os^{VI}(OEP)O$_2$ and Os^{VI}(TPP)O$_2$ (H$_2$OEP = octaethylporphyrin; H$_2$TPP = *meso*-tetraphenylporphyrin) with PPh$_3$ in CH$_2$Cl$_2$ yield Os^{II}(OEP)(OPPh$_3$)$_2$ (1) and Os^{II}(TPP)(PPh$_3$)$_2$ (2), respectively. The crystal structures of complexes 1 and 2 have been determined: 1·3H$_2$O, monoclinic, space group $P2_1/c$, a = 13.020 (2) Å, b = 14.474 (2) Å, c = 17.988 (3) Å, β = 103.36 (1)°, Z = 2; 2, triclinic, space group $P\bar{1}$, a = 11.536 (1) Å, b = 13.445 (1) Å, c = 21.237 (2) Å, α = 85.25 (1)°, β = 75.77 (1)°, γ = 69.55 (1)°, Z = 2. The Os–porphinato unit in 1 is planar within 0.07 Å, with Os–N = 2.029 (8) Å and Os–O(OPPh$_3$) = 2.036 (7) Å. The structure of 2 shows two independent, centrosymmetric molecules with Os–N = 2.044 (3) Å and Os–P = 2.148 (6) Å; the Os–porphinato groups are somewhat puckered, with out-of-plane deviations up to 0.12 Å. The Os–P distances in 2 are substantially longer than normal, reflecting the strong trans influence of PPh$_3$.

Introduction

We have begun a program of investigating oxygen atom transfer reactions of *trans*-dioxoosmium(VI) complexes.[2,3] The reactions of Os^{VI}(OEP)O$_2$ (H$_2$OEP = octaethylporphyrin) with PPh$_3$ in ROH (R = CH$_3$ or C$_2$H$_5$) were found to produce Os(OEP)-(OR)$_2$.[2] In CH$_2$Cl$_2$, PPh$_3$ reduction of Os(OEP)O$_2$ gives Os-(OEP)(OPPh$_3$)$_2$ (1) and PPh$_3$ reduction of Os(TPP)O$_2$ yields Os(TPP)(PPh$_3$)$_2$ (2) (H$_2$TPP = *meso*-tetraphenylporphyrin). The formation of Os(OEP)(OPPh$_3$)$_2$ from the reaction of Os(OEP)O$_2$ and PPh$_3$ implies that both Os(OEP)(O$_2$) and the presumed Os^{IV}(OEP)O(OPPh$_3$) intermediate are able to transfer an oxygen atom to PPh$_3$.[6] In this paper we describe the X-ray crystal structure characterization of these two new compounds. As far as we are aware, there are only two other structures reported for osmium porphyrins.[4,5]

Experimental Section

Octaethylporphyrin (H$_2$OEP), *meso*-tetraphenylporphyrin (H$_2$TPP), and Os$_3$(CO)$_{12}$ were obtained from Strem Chemicals. Os(OEP)O$_2$ and Os(TPP)O$_2$ were prepared as described previously.[2,6,7] All solvents and reagents were of analytical grade and used without further purification. UV–vis spectra were recorded on a Beckman Acta CIII spectrophotometer. Elemental analyses were performed by the Australian National Laboratory.

Bis(triphenylphosphine oxide)(octaethylporphinato)osmium(II), Os-(OEP)(OPPh$_3$)$_2$ (1). Method 1. Os(OEP)O$_2$ (100 mg, 0.13 mmol) and PPh$_3$ (200 mg, 0.76 mmol) were stirred in CH$_2$Cl$_2$ (50 mL) for 3 h. When all the dioxoosmium(VI) complex had reacted, as monitored by following the UV–vis spectral changes of the solution, the solvent was evaporated to ~2 mL at room temperature. The reaction product was purified by column chromatography on a silica column with CHCl$_3$ as eluant. The first orange-red band was Os(OEP)(PPh$_3$)$_2$ contaminated with some PPh$_3$. With acetone as the eluting solvent, a brown species was washed out. The desired product Os(OEP)(OPPh$_3$)$_2$ was finally eluted by methanol. The solvent was evaporated at room temperature, and the crude product was recrystallized as dark, air-stable plates from a CH$_2$Cl$_2$–cyclohexane mixture (1:1); yield 50%.

Method 2. Os(OEP)O$_2$ (50 mg, 0.07 mmol) and PPh$_3$ (60 mg, 0.22 mmol) in CH$_2$Cl$_2$ (200 mL) were irradiated with a 450-W high-pressure Hg short-arc lamp for 4 h.[8] The solvent was then evaporated, and the crude product was purified as described in method 1. UV–vis spectrum (CH$_2$Cl$_2$, λ_{max}/nm): 391, 454, 496, 506 sh, 536.

Bis(triphenylphosphine)(*meso*-tetraphenylporphinato)osmium(II), Os(TPP)(PPh$_3$)$_2$ (2). *trans*-[Os(TPP)O$_2$] (0.3 g, 0.36 mmol) and PPh$_3$ (1 g, 3.81 mmol) were stirred in a CH$_2$Cl$_2$–CH$_3$CN (1:1, 50 mL) mixture for 2 h. Violet, air-stable crystals of Os(TPP)(PPh$_3$)$_2$ gradually depositing upon standing; yield about 40%. Anal. Calcd for OsC$_{80}$H$_{58}$N$_4$P$_2$: C, 72.4; H, 4.4; N, 4.2; P, 4.7. Found: C, 72.3; H, 4.1; N, 4.2; P, 4.8. A ~10^{-6} M CH$_2$Cl$_2$ solution of Os(TPP)(PPh$_3$)$_2$ exhibits an intense Soret band at 408 nm.

Bis(triphenylphosphine)(octaethylporphinato)osmium(II). Reaction between Os(OEP)O$_2$ (0.1 g, 0.13 mmol) and PPh$_3$ (1 g, 3.81 mmol) in benzene (30 mL) at 50 °C for 2 h yielded Os(OEP)(PPh$_3$)$_2$. The UV–vis spectrum in benzene is similar to that of the well-characterized Os-(OEP)(PBu$_3$)$_2$[9] (λ_{max}/nm): 492, 516. Attempts to isolate an analytically pure sample of this compound were unsuccessful.

Crystal Structure Determination of Os(OEP)(OPPh$_3$)$_2$·3H$_2$O (1·3H$_2$O). Crystal Data: C$_{72}$H$_{80}$O$_5$N$_4$P$_2$Os, crystal size 0.22 × 0.34 × 0.08 mm, M_r = 1333.61, space group $P2_1/c$, a = 13.020 (2) Å, b = 14.474 (2) Å, c = 17.988 (3) Å, β = 103.36 (1)°, V = 3298.1 (15) Å^3 (21 °C),

(1) (a) University of Hong Kong. (b) California Institute of Technology. (c) On sabbatical leave at the California Institute of Technology.
(2) Che, C.-M.; Poon, C.-K.; Chung, W.-C.; Gray, H. B. *Inorg. Chem.* **1985**, *24*, 1277.
(3) Che, C.-M.; Cheng, W. K.; Mak, T. C. W. *Inorg. Chem.* **1986**, *25*, 703.
(4) Buchler, J. W.; Lam Lay, K.; Smith, P. D.; Scheidt, W. R.; Rupprecht, G. A.; Kenny, J. E. *J. Organomet. Chem.* **1976**, *110*, 109.
(5) Masuda, H.; Taga, T.; Osaki, K.; Sugimoto, H.; Mori, M. *Bull. Chem. Soc. Jpn.* **1984**, *57*, 2345.
(6) Recent work by Groves and co-workers suggests that Ru^{IV}(TMP)O (H$_2$TMP = tetramesitylporphyrin) disproportionates into Ru(II) and Ru(IV) in fluid solution: Groves, J. T.; Quinn, R. *J. Am. Chem. Soc.* **1985**, *107*, 5790.
(7) Buchler, J. W.; Smith, P. D. *Angew. Chem., Int. Ed. Engl.* **1974**, *13*, 341.
(8) Further information about the photochemical reactions of Os(OEP)O$_2$ with PPh$_3$ will be given later: Tang, W.-T.; Che, C.-M., manuscript in preparation.
(9) (a) Che, C.-M.; Chung, W.-C. *J. Chem. Soc., Chem. Commun.* **1986**, 386. (b) Buchler, J. W.; Smith, P. D. *Chem. Ber.* **1976**, *109*, 1465.

* To whom correspondence should be addressed.